Complexes of the Platinum Metals. Part 26.[1] Multinuclear Nuclear Magnetic Resonance Studies on Rhodium(II) Carboxylate Adducts

Esther B. Boyar and Stephen D. Robinson *
Department of Chemistry, King's College, Strand, London WC2R 2LS

A multinuclear (^{1}H, ^{13}C, ^{31}P, and ^{103}Rh), variable-temperature, n.m.r. study on some $[Rh_2(O_2CR)_4]$–$P(OR')_3$ systems (R = Me, Et, Pr, or Ph; R' = Me, Et, or Ph) is reported. The ambient-temperature (298 K) spectra, which generally display broad unresolved signals with no discernible internuclear couplings, are consistent with the establishment in solution of dynamic equilibria of the form $[\{(R'O)_3P\}Rh(O_2CR)_4Rh\{P(OR')_3\}] \rightleftharpoons [\{(R'O)_3P\}Rh(O_2CR)_4Rh(solv)] + P(OR')_3$ (solv = solvent). Low-temperature (*ca.* 213 K) spectra of the same solutions show fully resolved resonances indicative of a frozen equilibrium mixture containing mono and bis adducts together with free phosphorus-donor ligands. The large ^{31}P chemical shift difference (*ca.* 50—60 p.p.m.) between the mono and bis adducts points to the operation of a strong *trans* influence across the binuclear metal centre. This has been confirmed by a study of *ca.* 30 mixed adducts $[\{(MeO)_3P\}Rh(O_2CMe)_4RhL]$ in which ^{31}P chemical shifts and $^2J(RhP)$ coupling constants have been employed to establish a *trans*-influence series for the ligands L.

Since their discovery and subsequent structural characterisation by Chernyaev *et al.*[2] over 20 years ago, the binuclear rhodium(II) carboxylates $[Rh_2(O_2CR)_4]$ have attracted and sustained a remarkably high level of interest. A programme of synthesis, conducted largely by Russian chemists, has afforded a vast array of solvates $[Rh_2(O_2CR)_4(solv)_2]$, adducts $[Rh_2(O_2CR)_4L_n]$ (n = 1 or 2), and salts $M_n[Rh_2(O_2CR)_4X_n]$ (n = 1 or 2).[3,4] At the same time, interest in the novel 'lantern' structure and its associated Rh–Rh axial interaction has fostered an intensive study of the magnetic, spectroscopic, and electronic properties of these systems which in turn have fuelled a fierce controversy concerning the nature of the axial Rh–Rh and Rh–L (or X) bonds.[3,4] More recently, reports that rhodium(II) carboxylato-complexes display significant anti-tumour activity [5] have led to thermodynamic [6—11] and kinetic studies [6] on ligand-dissociation and exchange processes.

However, given the high stability and symmetry of the 'lantern' structures and the presence of several magnetically active nuclei in close proximity within these molecules, surprisingly little n.m.r. work has been reported on rhodium(II) carboxylates. In addition to a few papers which simply record data, there are reports on the application of n.m.r. spectroscopy in the identification of co-ordination sites in ambidentate ligands (*i.e.* adenine and adenosine),[12,13] the investigation of carboxylate ligand exchange ($MeCO_2^-$–$CF_3CO_2^-$),[14,15] and the determination of magnetic moments (Evans' method) in the rhodium(II, III) systems $[Rh_2(O_2CR)_4]^+$.[16]

The apparent neglect of this promising field of study led to the initiation of a multinuclear n.m.r. investigation the first fruits of which are reported in the present paper.[17] In order to maximise the range of information obtainable the P-donor adducts $[Rh_2(O_2CR)_4\{P(OR')_3\}_2]$ were chosen for this initial study.

Experimental

The complexes $[Rh_2(O_2CR)_4(solv)_2]$ were prepared by literature methods [18—20] and were desolvated by gentle heating *in vacuo*. Adducts $[Rh_2(O_2CR)_4\{P(OR')_3\}_2]$ were obtained by adding neat ligand $P(OR')_3$ to the appropriate rhodium(II) carboxylate in the solid state or in diethyl ether suspension until the colour change from green to orange was complete, and were stored under nitrogen. 'Aged' samples gave solutions containing significant amounts of the corresponding trialkyl phosphate ester. The mixed adducts $[Rh_2(O_2CR)_4\{P(OR')_3\}L]$ were prepared *in situ* by adding the free ligand L to a solution of $[Rh_2(O_2CR)_4\{P(OR')_3\}_2]$ and $[Rh_2(O_2CR)_4]$ (1 : 1 molar ratio) in the n.m.r. solvent.

The ^{1}H n.m.r. spectra were recorded at 250 MHz on a Bruker WM 250 spectrometer operating at 298 and 213 K. Solutions in CD_2Cl_2 were measured in 5-mm tubes with pulsed Fourier transform. Peak positions were measured in p.p.m. from $SiMe_4$ as the internal standard. Other parameters were: pulse width, 1 µs; 16K data points; sweep width, 3 000 Hz; 4 400 Hz offset; 32—64 scans.

The ^{31}P n.m.r. spectra were recorded at 36.4 MHz on a Bruker HFX 90 spectrometer operating at 298 K and at various temperatures down to 213 K. Solutions in CD_2Cl_2 were measured in 10-mm tubes with broad-band decoupling and pulsed Fourier transform. Peak positions were measured in p.p.m. from 85% H_3PO_4 as the external standard. Other parameters were: pulse width, 75 µs; 8 500 Hz offset; 1 024—4 096 scans.

The ^{13}C n.m.r. spectra were recorded at 22.63 MHz on a Bruker HFX 90 spectrometer operating at 298 and 213 K. Solutions in CD_2Cl_2 were measured in 10-mm tubes with broad-band decoupling and pulsed Fourier transform. Peak positions were measured in p.p.m. from $SiMe_4$ as internal standard. Other parameters were: pulse width, 10 µs; 4K data points; time constant 2 s; sweep width, 5 435 Hz; 6 750 Hz offset; 1 900—3 317 scans.

The ^{103}Rh spectrum was recorded on a Bruker WH-400 spectrometer operating at 12.58 MHz at 243 K. Solutions in CD_2Cl_2 were measured in 10-mm tubes with pulsed Fourier transform. Peak positions were measured in p.p.m. from $\Xi(^{103}Rh)$ = 3.16 MHz. Other parameters were: pulse width, 10 µs; 64K data points, line broadening, 10 Hz; sweep width, 100 000 Hz; 20 000 Hz offset; 156 073 scans.

All spectra were recorded with positive shifts to low field of the reference.

Results and Discussion

The n.m.r. spectra (^{1}H, ^{13}C, ^{31}P, and ^{103}Rh) of '$[Rh_2(O_2CMe)_4\{P(OMe)_3\}_2]$' in CD_2Cl_2 solution can be interpreted in terms of mono and bis adducts (1a) and (1b), free trimethyl phosphite, and traces of extraneous trimethyl phosphate. The last species is apparently formed by aerobic oxidation of the free phosphite in solution. At ambient temperature (298 K) the ^{1}H and ^{31}P-{^{1}H} n.m.r. spectra display broad unresolved

Table 1. ^{31}P N.m.r. data for adducts $[Rh_2(O_2CR)_4\{P(OR')_3\}_n]$ (n = 1 or 2)

			213 K			
		298 K singlet	AA′XX′ pattern (n = 2)	AMX pattern (n = 1)		
R	R′	(δ/p.p.m.)	(δ/p.p.m.)	δ/p.p.m.	$^1J(RhP)$/Hz	$^2J(RhP)$/Hz
Me	Me	91.9	93.5 [a]	36.7	151.4	43.9
Me	Et	92.75	90.2	34.05	147.7	42.7
Me	Ph	73.18	73.6	17.29	147.7	57.4
Et	Me	95.03	95.13	*b*		
Pr	Me	93.69	93.99	38.50	192.9	44.0
Ph	Me	95.06	94.99	38.03	149.0	39.1

[a] Computer simulation using data extracted from the ^{31}P and ^{103}Rh spectra gave the following coupling constants: $^1J(RhP)$ = 134, $^2J(RhP)$ = −1.5, $^3J(PP')$ = 853, and $^1J(RhRh)$ = 7.9 Hz. [b] Signal visible but weak and poorly resolved.

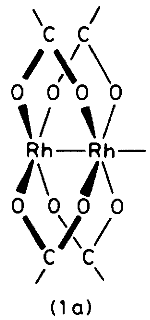

(1a)

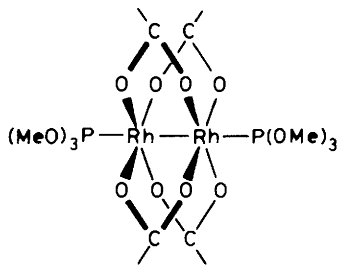

(1b)

signals with no discernible evidence of internuclear coupling. Only the ^{13}C-{^1H} spectrum, where an isotope-dilution effect is evident, shows sharply resolved resonances. Data recorded under these conditions are: ^1H, $\delta(CH_3CO_2)$ 1.83(s) and $\delta[P(OCH_3)_3]$ 3.89(s); ^{13}C-{^1H}, $\delta(CH_3CO_2)$ 24.13(s), $\delta(CH_3CO_2)$ 193.12(s), and $\delta[P(OCH_3)_3]$ 51.28(s); ^{31}P-{^1H}, $\delta[P(OCH_3)_3]$ 91.9(s) p.p.m. These spectra are consistent with a rapid dissociative equilibrium of the form $[\{(MeO)_3P\}Rh(O_2CMe)_4Rh\{P(OMe)_3\}] \rightleftharpoons [\{(MeO)_3P\}Rh(O_2CMe)_4Rh(solv)] + P(OMe)_3$. A process of this type is very feasible since the axial ligands, L, in adducts of the form $[Rh_2(O_2CR)_4L_2]$ are known to be highly substitution labile. Alternative explanations for the broad nature of the n.m.r. spectra involving carboxylate-exchange processes can readily be discounted since the carboxylate bridges in these complexes are known to be relatively inert. Thus, rate constants, k_1—k_4, for the stepwise replacement of acetate by trifluoroacetate in $[Rh_2(O_2CMe)_4]$ have been given as 7.2×10^{-4}, 1.4×10^{-3}, 6×10^{-5}, and 2×10^{-5} s^{-1} respectively.[14] On cooling the solution to 213 K the free and bound trimethyl phosphite-exchange process is frozen out; under these conditions sharp signals attributable to mono and bis adducts (1a) and (1b) appear with well defined intramolecular couplings.

The low-temperature ^1H n.m.r. spectrum comprises a singlet at 1.92 (CH_3CO_2) and a doublet at 3.92 p.p.m., $^3J(PH)$ = 11.0 Hz $[P(OCH_3)_3]$ attributable to the mono adduct (1a) together with a singlet at 1.87 p.p.m. (CH_3CO_2) and a virtual-coupling triplet pattern at 3.88 p.p.m., N = 11.0 Hz $[P(OCH_3)_3]$, arising from the bis adduct (1b). A doublet at 3.78 p.p.m., $^3J(PH)$ = 11.0 Hz, is assigned to traces of trimethyl phosphate. On addition of excess of trimethyl phosphite (*ca.* 4 mol per mol of dimer) the signals due to the mono adduct disappear and a new doublet pattern [δ 3.51 p.p.m., $^3J(PH)$ = 10.3 Hz] attributable to the excess of free phosphite is observed. There is no evidence of $J(RhH)$ coupling in these spectra.

The low-temperature ^{13}C-{^1H} n.m.r. spectrum contains singlets at δ 23.97 (CH_3CO_2), 191.60 (CH_3CO_2), and 51.59 p.p.m. $[P(OCH_3)_3]$ attributed to the mono adduct, together with resonances at 24.20 (CH_3CO_2), 193.56 (CH_3CO_2), and 50.74 p.p.m. $[P(OCH_3)_3]$ arising from the bis adduct. The CH_3CO_2 ^{13}C resonance of the bis adduct displays a small triplet splitting, $^3J(CP)$ = *ca.* 8 Hz, but there is no visible evidence of a similar coupling for the mono adduct. The absence of discernible coupling between the ^{13}C and ^{31}P nuclei of the trimethyl phosphite ligands can be attributed to the algebraic cancellation of $^2J(CP)$ and $^5J(CP)$. A similar phenomenon has previously been reported for the complexes *cis*-$[MCl_2\{P(OMe)_3\}_2]$ (M = Pd or Pt) where $^2J(CP)$ and $^4J(CP)$ are of equal magnitude but opposite sign, and cancel algebraically.[21]

The ^{31}P-{^1H} spectra, recorded at 213 K, consist of the X portion of an AMX pattern and the XX′ portion of an AA′-XX′ pattern (A, A′, and M = ^{103}Rh; X, X′ = ^{31}P) arising from the mono and bis adducts respectively. Data obtained by first-order analysis of the AMX pattern and computer simulation of the AA′XX′ pattern are as follows: mono adduct (AMX pattern), δ 36.70 p.p.m., $^1J(RhP)$ 151.4, $^2J(RhP)$ 43.9 Hz; bis adduct (AA′XX′), δ 93.5 p.p.m., $^1J(RhP)$ 134, $^2J(RhP)$ −1.5, $^3J(PP')$ 853 Hz.

The low-temperature ^{103}Rh spectrum of the bis adduct consists of a broad but well defined virtual-coupling triplet pattern δ 6 694 p.p.m. (N = 137.3 Hz). This spectrum is reproduced in the preliminary communication.[17a] The ^{103}Rh signal of the mono adduct could not be resolved.

Similar spectra have been recorded for a series of carboxylates $[Rh_2(O_2CR)_4\{P(OMe)_3\}_2]$ (R = Me, Et, Pr, or Ph). The ambient-temperature ^1H n.m.r. spectra are all consistent with the rapid exchange of free and bound trimethyl phosphite ligands whilst the low-temperature (213 K) spectra show a doublet and a virtual-coupling triplet due to the $P(OCH_3)_3$ protons of the mono and bis adducts respectively. The ambient-temperature ^{31}P-{^1H} spectra each display a broad singlet at *ca.* 90—95 p.p.m.; on cooling the samples to 213 K

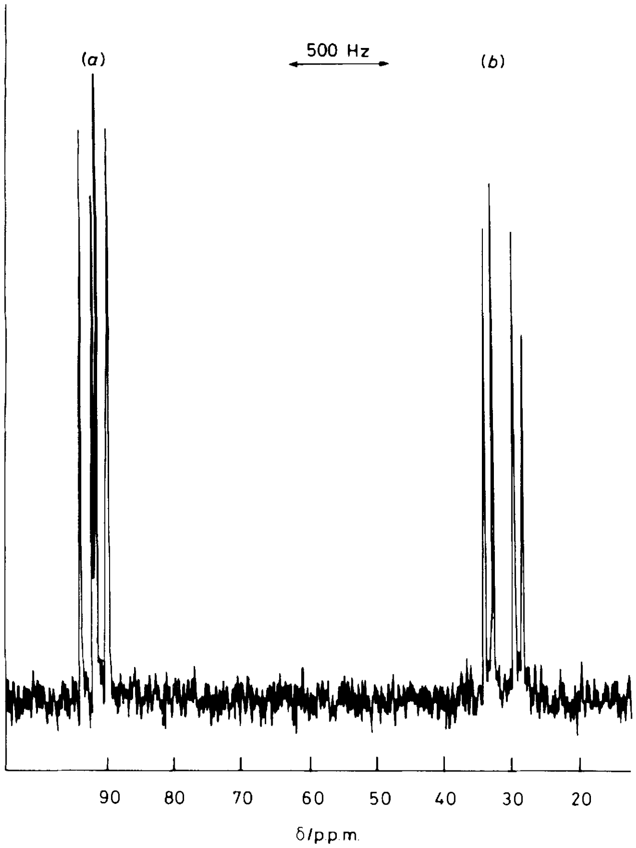

Figure 1. $^{31}P-\{^1H\}$ N.m.r. spectrum of $[Rh_2(O_2CMe)_4]-P(OMe)_3$ system: (*a*) bis adduct; (*b*) mono adduct

each spectrum consists of the X portion of an AMX pattern (*ca.* 37 p.p.m.) and the XX′ portion of an AA′XX′ pattern (*ca.* 94 p.p.m.) attributable to mono and bis adducts respectively. Similar behaviour was observed when other phosphite ligands $P(OR)_3$ (R = Et or Ph) were employed. Phosphorus-31 data are recorded in Table 1. However, attempts to prepare and study phosphite adducts of $[Rh_2(O_2CCF_3)_4]$ were frustrated by an apparent redox reaction. Addition of $P(OMe)_3$ to a solution of $[Rh_2(O_2CCF_3)_4]$ in CD_2Cl_2 immediately produced the orange colour anticipated for a phosphite adduct. However, this rapidly faded to leave a lemon yellow solution the $^{31}P-\{^1H\}$ n.m.r. spectrum of which was temperature independent and showed two doublets (δ 131.55 and 71.97 p.p.m.) with $^1J(RhP)$ couplings (205.1 and 170.9 Hz respectively) indicative of rhodium(I) species. Attempts to isolate crystalline products from these yellow solutions were unsuccessful.

The large chemical shift difference (*ca.* 57 p.p.m.) observed in the low-temperature (213 K) $^{31}P-\{^1H\}$ n.m.r. spectra of the $[Rh_2(O_2CMe)_4]-P(OMe)_3$ system between the signals of the bis adduct (*ca.* 94 p.p.m.) and those of the mono adduct (*ca.* 37 p.p.m.) clearly indicated the presence of a strong *trans* influence operating across the binuclear rhodium(II) centre. In view of the current interest in binuclear metal centres, $[M_2(O_2CR)_4L_2]$,[3,4] and the paucity of data on *trans* influences operating along the axis of such systems we undertook a qualitative study of this phenomenon using the mixed adducts $[\{(MeO)_3P\}Rh(O_2CMe)_4RhL]$. Solutions of the mixed adducts, prepared by adding the free ligand, L, to mixtures of $[Rh_2(O_2CMe)_4\{P(OMe)_3\}_2]$ and $[Rh_2(O_2CMe)_4]$ in CD_2Cl_2, were examined by $^{31}P-\{^1H\}$ n.m.r. spectroscopy at 213 K. In each case the spectrum, which was similar in form to that illustrated in Figure 1, consisted of the XX′ portion of an AA′XX′ pattern attributable to the bis adduct $[Rh_2(O_2CMe)_4\{P(OMe)_3\}_2]$ and an AMX pattern arising from the mixed adduct $[\{(MeO)_3P\}Rh(O_2CMe)_4RhL]$. The third component of the mixture $[Rh_2(O_2CMe)_4L_2]$ is ^{31}P n.m.r. silent except in those cases where L is a P-donor ligand (see below). In this manner *ca.* 30 mixed adducts in which L is a P, As, Sb, Bi, N, S, or O donor ligand have been investigated (Table 2). A plot of the ^{31}P n.m.r. chemical shifts recorded for the mixed adducts [δ(AMX)] *versus* the coupling constants $^2J(RhP)$ reveals a good linear inverse correlation between the two parameters (Figure 2). The sequence of ligands, L, generated by the plot constitutes a *trans*-influence series: $P(OMe)_3 > P(OPh)_3 \approx PPh_3 > AsPh_3 > SbPh_3 \approx$ pyridine (py) $> NHEt_2 > NEt_3 > NH_2Ph > NCO^- > MeCN \approx PhCN > MeNCS > BiPh_3 > H_2O \approx Me_2CO \approx$ tetrahydrofuran (thf).

Table 2. ^{31}P N.m.r. data for 'mixed' adducts $[Rh_2(O_2CMe)_4L\{P(OMe)_3\}]$

L	δ/p.p.m. (AMX Pattern *)	$^2J(RhP)$/ Hz	$^1J(RhP)$/ Hz
Me_3CNC	81.82	<10	136.70
$AsPh_3$	71.30	12.20	144.05
$C_5H_{10}NH$	68.58	20.75	137.95
$MeSC_3H_5$	68.15	18.30	142.80
C_4H_8S	68.12	19.55	144.05
Me_2SO	67.21	17.10	144.05
2-HSC_5H_4N	65.61	17.10	144.05
CO	64.77	24.40	136.70
4-MeC_5H_4N	64.77	19.55	139.15
C_5H_5N	64.75	19.55	139.15
NH_2Me	64.46	19.50	139.15
$SbPh_3$	63.95	15.85	145.25
$NHEt_2$	62.89	23.65	137.95
$PhSC_3H_5$	61.65	21.95	144.05
NEt_3	56.09	25.65	137.95
p-$MeC_6H_4NH_2$	55.69	28.10	142.80
NH_2Ph	53.06	30.50	145.25
NCO^-	51.25	31.00	137.60
PPh_3S	49.88	30.50	147.70
$CH_2=CHCN$	49.26	26.85	144.05
MeCN	49.09	26.85	141.60
PhSH	49.02	31.75	146.50
PhCN	48.75	26.85	141.60
MeNCS	45.00	36.60	146.50
Bu^t_2S	42.52	36.60	146.50
CS_2	41.05	41.50	151.4
C_4H_4S	40.58	39.05	151.35
$BiPh_3$	40.00	41.50	148.95
SO_2	37.66	45.15	150.15
C_4H_8O	36.84	42.70	150.15
H_2O	36.70	43.90	151.40
Me_2CO	36.08	42.70	147.70

* In each spectrum the ^{31}P resonance of $[Rh_2(O_2CMe)_4\{P(OMe)_3\}_2]$ appears at *ca.* 92.5 p.p.m. Small variations (± 1 p.p.m.) are attributed to solvent effects arising from the presence of significant concentrations of the various free ligands L. All spectra taken at 213 K.

Data for S-donor ligands generate points which fall on or near the straight line plot but the δ(AMX) and $^2J(RhP)$ values recorded span wide ranges (*ca.* 30 p.p.m. and 20 Hz respectively) and thus imply large differences in the magnitudes of the *trans* influences exerted by the various S-donor ligands concerned. These in turn presumably reflect the variations in steric hindrance (Bu^t_2S *vs.* C_4H_8S) and sulphur oxidation state (Bu^t_2S *vs.* Me_2SO) or hybridisation (Me_2SO *vs.* CS_2) found amongst the S-donor ligands employed. The almost total absence of anionic ligands in our *trans*-influence series reflects technical problems. Chief amongst these was the lack of a suitable n.m.r. solvent capable of maintaining the mixed salts $M[\{(MeO)_3P\}Rh(O_2CMe)_4RhX]$ in solution at the low temperature required to freeze out the ligand-dissociation process. The ^{31}P-{^{1}H} n.m.r. spectra of mixed P-donor adducts are more complex than those observed for systems where L is a non-P donor. This point is illustrated by the ^{31}P-{^{1}H} spectrum of the $[Rh_2(O_2CMe)_4\{P(OMe)_3\}_2]$–$[Rh_2(O_2CMe)_4]$–$PPh_3$ system reproduced in Figure 3. In addition to free triphenylphosphine (not shown), three rhodium-bearing species $[Rh_2(O_2CMe)_4\{P(OMe)_3\}_2]$, $[Rh_2(O_2CMe)_4(PPh_3)_2]$, and $[Rh_2(O_2CMe)_4(PPh_3)\{P(OMe)_3\}]$ are present in the mixture and each displays a clearly resolved ^{31}P-{^{1}H} n.m.r. pattern. The bis(trimethyl phosphite) adduct generates the XX′ portion of the AA′XX′ pattern as discussed above. A similar pattern is also observed for the bis(triphenylphosphine) adduct, however this complex has rather low solubility and for this reason we have been unable to record the ^{103}Rh spectrum necessary for a complete analysis. The mixed PPh_3–$P(OMe)_3$ adduct displays an eight-line ^{31}P-{^{1}H} n.m.r. spectrum in which the two non-equivalent ^{31}P nuclei present each generates a doublet of doublets pattern. Both patterns display essentially first-order behaviour (spectra run at 36.44 and 101.2 MHz) and were accordingly analysed as the P and X components of an AMPX pattern in which the couplings $^2J(RhP)$ are both equal to zero. Data obtained in this manner for the mixed adduct are: $\delta\{P(OMe)_3\}$ 87.0 p.p.m., $^1J(RhP)$ 141.6, $^3J(PP')$ 525.5 Hz; $\delta(PPh_3)$ $-$ 18.32 p.p.m., $^1J(RhP)$ 84.2, $^3J(PP')$ 525.5 Hz.

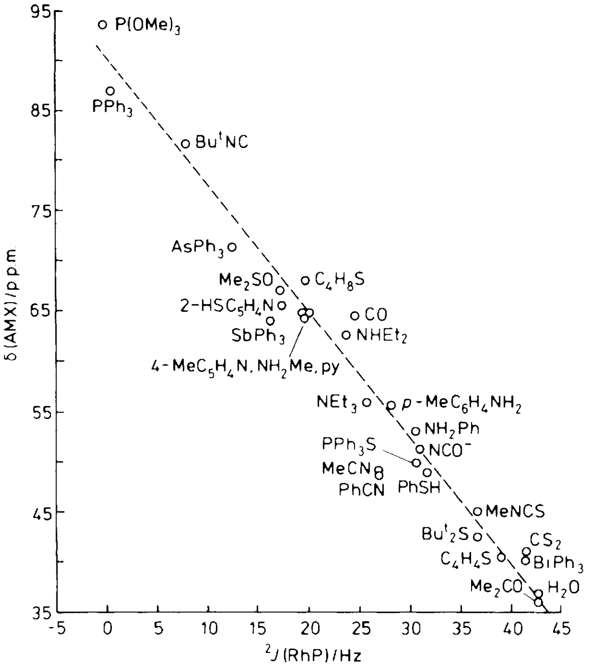

Figure 2. Plot of ^{31}P chemical shifts δ(AMX) *versus* the coupling constants $^2J(RhP)$ for mixed adducts $[\{(MeO)_3P\}Rh(O_2CMe)_4RhL]$

A roughly linear correlation exists between the magnitudes of the ^{31}P chemical shifts recorded for the various mixed L–$P(OMe)_3$ adducts and the Rh–Rh distances found for the corresponding bis adducts $[Rh_2(O_2CMe)_4L_2]$ where these are known (Figure 4). It follows from this observation and the data discussed earlier that there is an approximately linear

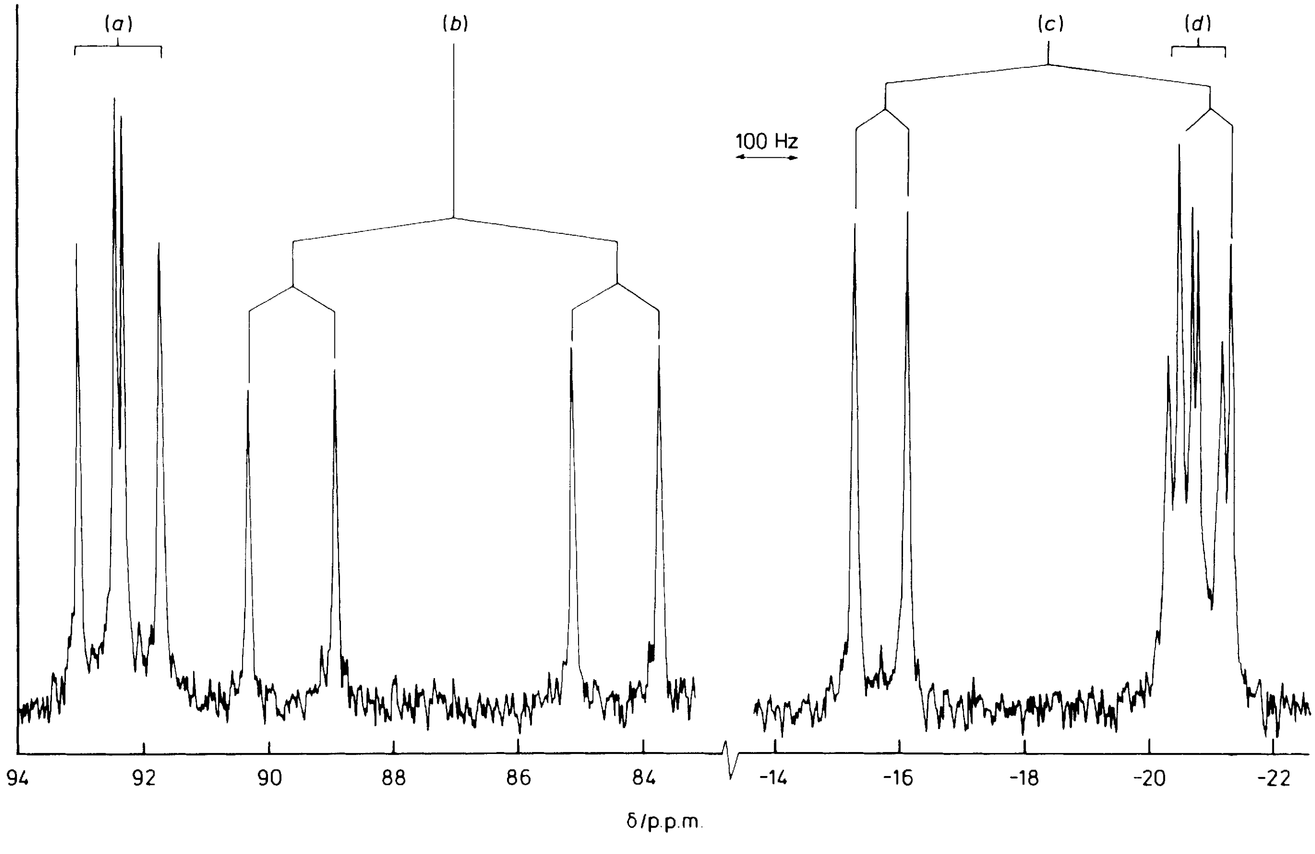

Figure 3. ^{31}P-{^{1}H} N.m.r. spectrum of the $[Rh_2(O_2CMe)_4]$–$P(OMe)_3$–PPh_3 system: (*a*) $[Rh_2(O_2CMe)_4\{P(OMe)_3\}_2]$; (*b*) $[(Ph_3P)Rh(O_2CMe)_4Rh\{P(OMe)_3\}]$; (*c*) $[(Ph_3P)Rh(O_2CMe)_4Rh\{P(OMe)_3\}]$; and (*d*) $[Rh_2(O_2CMe)_4(PPh_3)_2]$

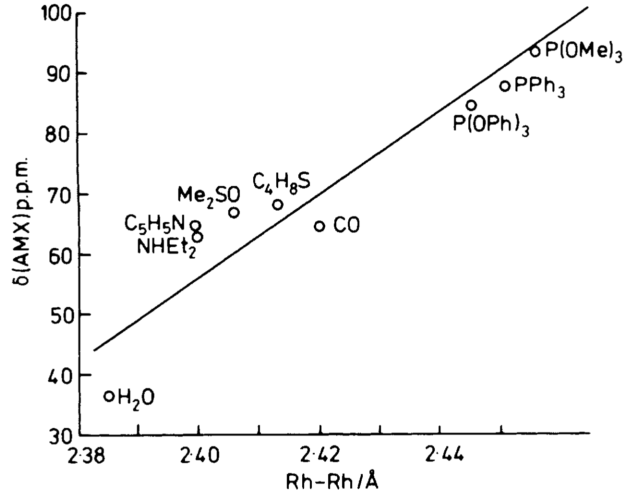

Figure 4. Plot of the ^{31}P n.m.r. chemical shift for 'mixed' adducts [$Rh_2(O_2CMe)_4L\{P(OMe)_3\}$] *versus* the Rh–Rh bond lengths for the corresponding bis adducts [$Rh_2(O_2CMe)_4L_2$]

inverse correlation between the Rh–Rh distances and the values of ^2J(RhP).

Although there is still some controversy concerning the nature of the Rh–Rh and, in particular, Rh–P axial bonds in P-donor adducts [$Rh_2(O_2CR)_4(PR_3)_2$] the general consensus appears to be that π-bonding contributions are of little significance.[22] It is therefore not surprising that the ligand sequence established in the present work closely parallels *trans*-influence series constructed, using similar n.m.r. data, for various classes of mononuclear complexes, in particular the square-planar platinum(II) species *trans*-[$PtR(X)(PR'_3)_2$] and *trans*-[$PtR(L)(PR'_3)_2$] (R = H or CH_3) in which σ-bonding effects are dominant.[23,24]

Acknowledgements

We thank Dr. B. E. Mann for obtaining the ^{103}Rh n.m.r. spectrum, the S.E.R.C. for financial support (to E. B. B.), and the University of London Central Research Fund for financing the purchase of rhodium trichloride.

References

1 Part 26, E. B. Boyar, A. Dobson, S. D. Robinson, B. L. Haymore, and J. C. Huffman, preceding paper.
2 I. I. Chernyaev, E. V. Shenderetskaya, and A. A. Karyagina, *Zh. Neorg. Khim.*, 1960, **5**, 1163; *Russ. J. Inorg. Chem.*, 1960, **5**, 559.
3 E. B. Boyar and S. D. Robinson, *Coord. Chem. Rev.*, 1983, **50**, 109.
4 T. R. Felthouse, *Prog. Inorg. Chem.*, 1982, **29**, 73.
5 R. G. Hughes, J. L. Bear, and A. P. Kimball, *Proc. Am. Assoc. Cancer Res.*, 1972, **13**, 120.
6 J. L. Bear, R. A. Howard, and J. E. Korn, *Inorg. Chim. Acta*, 1979, **32**, 123.
7 K. Das and J. L. Bear, *Inorg. Chem.*, 1976, **15**, 2093.
8 K. Das, E. L. Simmons, and J. L. Bear, *Inorg. Chem.*, 1977, **16**, 1268.
9 A. M. Dennis, R. A. Howard, and J. L. Bear, *Inorg. Chim. Acta*, 1982, **66**, L31.
10 L. Rainen, R. A. Howard, A. P. Kimball, and J. L. Bear, *Inorg. Chem.*, 1975, **14**, 2752.
11 R. S. Drago, J. R. Long, and R. Cosmano, *Inorg. Chem.*, 1981, **20**, 2920.
12 G. Pneumatikakis and N. Hadjiliadis, *J. Chem. Soc., Dalton Trans.*, 1979, 596.
13 K. Aoki and H. Yamazaki, *J. Chem. Soc., Chem. Commun.*, 1980, 186.
14 J. L. Bear, J. Kitchens, and M. R. Willcott, *J. Inorg. Nucl. Chem.*, 1971, **33**, 3479.
15 J. L. Bear, H. B. Gray, L. Rainen, I. M. Chang, R. A. Howard, G. Serio, and A. P. Kimball, *Cancer Chemother. Rep.*, 1975, **59**, 611.
16 C. R. Wilson and H. Taube, *Inorg. Chem.*, 1975, **14**, 2276.
17 (*a*) E. B. Boyar and S. D. Robinson, *Inorg. Chim. Acta*, 1982, **64**, L193; (*b*) *ibid.*, 1983, **76**, L137.
18 P. Legzdins, R. W. Mitchell, G. L. Rempel, J. D. Ruddick, and G. Wilkinson, *J. Chem. Soc. A*, 1970, 3322.
19 R. S. Drago, S. P. Tanner, R. M. Richman, and J. R. Long, *J. Am. Chem. Soc.*, 1979, **101**, 2897.
20 J. Kitchens and J. L. Bear, *Thermochim. Acta*, 1970, **1**, 537.
21 A. W. Verstuyft, J. H. Nelson, and L. W. Cary, *Inorg. Chem.*, 1976, **15**, 732.
22 B. E. Bursten and F. A. Cotton, *Inorg. Chem.*, 1981, **20**, 3042.
23 T. Miyamoto, *J. Organomet. Chem.*, 1977, **134**, 335.
24 T. G. Appleton and M. A. Bennett, *Inorg. Chem.*, 1978, **17**, 738.

Received 9*th March* 1984; *Paper* 4/390